Alkalinity modulates a unique suite of genes to recalibrate growth and pH homeostasis

Mitylene Bailey[1], En-Jung Hsieh[1], Huei-Hsuan Tsai[1†],
Arya Ravindran[1] and Wolfgang Schmidt[1,2,3]*

[1]Institute of Plant and Microbial Biology, Academia Sinica, Taipei, Taiwan, [2]Biotechnology Center,
National Chung-Hsing University, Taichung, Taiwan, [3]Genome and Systems Biology Degree Program,
College of Life Science, National Taiwan University, Taipei, Taiwan

Alkaline soils pose a conglomerate of constraints to plants, restricting the growth and fitness of non-adapted species in habitats with low active proton concentrations. To thrive under such conditions, plants have to compensate for a potential increase in cytosolic pH and restricted softening of the cell wall to invigorate cell elongation in a proton-depleted environment. To discern mechanisms that aid in the adaptation to external pH, we grew plants on media with pH values ranging from 5.5 to 8.5. Growth was severely restricted above pH 6.5 and associated with decreasing chlorophyll levels at alkaline pH. Bicarbonate treatment worsened plant performance, suggesting effects that differ from those exerted by pH as such. Transcriptional profiling of roots subjected to short-term transfer from optimal (pH 5.5) to alkaline (pH 7.5) media unveiled a large set of differentially expressed genes that were partially congruent with genes affected by low pH, bicarbonate, and nitrate, but showed only a very small overlap with genes responsive to the availability of iron. Further analysis of selected genes disclosed pronounced responsiveness of their expression over a wide range of external pH values. Alkalinity altered the expression of various proton/anion co-transporters, possibly to recalibrate cellular proton homeostasis. Co-expression analysis of pH-responsive genes identified a module of genes encoding proteins with putative functions in the regulation of root growth, which appears to be conserved in plants subjected to low pH or bicarbonate. Our analysis provides an inventory of pH-sensitive genes and allows comprehensive insights into processes that are orchestrated by external pH.

KEYWORDS

alkaline soils, pH homeostasis, root growth, bicarbonate, iron acquisition, nitrate uptake

Introduction

Soil pH, a composite readout derived from weathering, climate, vegetation, and the parental material, exerts a multitude of effects on the plant's productivity and fitness. While the concentration of hydrogen ions can vary both spatially and temporally, the pH of the soil solution is characteristic of a certain habitat and soil type, and governs the composition of natural plant communities by defining the availability of nutrients, the activity of soil microbial assemblages, the seed germination rate, and the available water capacity (Tsai and Schmidt, 2021). Soil pH can range from extreme acidic (~pH 3) to extreme alkaline (~pH 9) conditions. In acid soils, the presence of Al^{3+}, released from clay minerals at a pH below 5 is the main factor that restricts species with insufficient detoxification mechanisms to thrive under such conditions. Alkaline soils, on the other hand, dramatically limit the availability of iron and phosphate, excluding so-called calcifuge (chalk-fleeing) species from these habitats. Interestingly, in sorghum, tolerance to alkalinity is dependent on H_2O_2 homeostasis, which was shown to be controlled by an atypical G protein γ subunit referred to as *Alkaline tolerance 1* (*AT1*) (Zhang et al., 2023). AT1 is phosphorylating the aquaporin PIP2 on the plasma membrane, which compromises the export of H_2O_2 by PIP2 and decreases growth performance on alkaline media. Alkaline calcareous soils contain high levels of calcium or magnesium carbonate that both increase and buffer soil pH, posing a further constraint on plants growing on such sites. Calcicole (chalk-loving) species that can tolerate these conditions are able to efficiently mine iron and phosphate from recalcitrant pools (Grime and Hodgson, 1968). If —or to what extent—pH as such plays a role in defining calcicole behavior is not known.

Maintaining cytosolic pH within a narrow, slightly alkaline set value is critical to cell viability. To recalibrate intracellular proton concentration, plant cells employ a mechanism referred to as the biochemical pH stat (Smith and Raven, 1979), which depends on the production or consumption of protons during the carboxylation and decarboxylation of organic acids. In addition, electrogenic transport processes driven by plasma membrane-localized P-type and vacuolar V-ATPases contribute to cellular pH homeostasis, a regulatory mechanism referred to as biophysical pH stat. Migration of protons across the plasma membrane alters, however, both the cytoplasmic and apoplastic pH. While the cytosol features a neutral to slightly alkaline pH, the apoplast of plant cells is more acidic and characterized by intricate pH gradients between the plasma membrane and the outer surface of the root cells as well as radially across different root tissues (Martinière et al., 2018). Growth of plant cells is associated with substantial remodeling of the rigid cell walls surrounding the cytoplasm (Cosgrove, 2018), a process that is strongly dependent on pH. An acidic apoplast is a prerequisite for loosening the cell wall to aid cell elongation (acid growth theory; Hager et al., 1971). Acidification of the apoplast is mediated by ATPases that pump H^+ from the cytosol into the apoplast. Alkalinity, by contrast, compromises growth by rigidifying the cell wall. Rapid alkalinization factor (RALF) peptides bind to the cell surface receptor kinase FERONIA (FER) and counteract acidification of the cell wall pH by inhibiting H^+-ATPases,

reversibly suppressing cell elongation (Pearce et al., 2001; Gjetting et al., 2020). Notably, RALF-FER was shown to interact with auxin signaling by upregulating auxin biosynthesis and signaling, adjusting root growth in response to environmental stimuli (Li et al. (2022). Crucially, changing apoplastic pH—either by manipulating electrogenic proton fluxes across the plasma membrane or by exposing plants to media of different pH—alters root growth according to the prevailing hydrogen concentration (Li et al., 2021; Lin et al., 2021), corroborating this concept.

If and how plants sense the pH of the apoplast was a long-standing enigma (Tsai and Schmidt, 2021). Recently, a bimodal apoplastic pH sensing system was shown to negotiate the balance of two basic tasks of root cells, growth and defense (Liu et al., 2022a). In this system, a sulfotyrosine residue in the root growth factor (RGF) peptide is protonated at low pH, which facilitates binding to its receptor RGFR and supports meristem development by regulating PLETHORA protein gradients (Aida et al., 2004; Liu et al., 2022a). At elevated pH this residue is deprotonated, which compromises the formation of the RGF-RGFR complex. Alkalization of the apoplast engages a second component of the pH sensing system by removing protons from essential Glu and Asp residues of the receptor protein PEPR, which supports binding of its ligand PEP1 and triggers immunity.

Whether the RGF/PEP-based sensing system is also critical for the adaptation of plants to alkaline conditions remains to be elucidated. To shed light on the mechanisms that allow perception of external pH and pH-dependent adjustment of metabolism and growth, we conducted gene expression analyses of (calcifuge) *Arabidopsis* plants subjected to alkaline conditions. In addition, we analyzed the growth of plants exposed to media differing in pH, including a treatment where external pH was controlled by supplementing the growth media with bicarbonate. We hypothesized that short-term exposure to high pH engages or repress signaling cascades and transport processes that adapt plants to alkaline conditions. Employing transcriptomic analysis and a comparison with related transcriptomic studies, we aimed at disclosing genes and putative gene modules with putative roles in intracellular pH homeostasis and root development.

Materials and methods

Plant growth conditions

Seeds of Arabidopsis (*A. thaliana* (L.) Heynh) accession Col-0 were obtained from the Arabidopsis Biological Resource Center (Ohio State University). Seeds were sterilized with 35% (v/v) bleach, washed five times with sterile water. Plants were grown in a growth chamber on solid nutrient media as described by Estelle and Somerville (1987) (ES media), composed of 5 mM KNO_3, 2 mM $MgSO_4$, 2 mM $Ca(NO_3)_2$, 2.5 mM KH_2PO_4, 70 μmM H_3BO_3, 14 μM $MnCl_2$, 1 μM $ZnSO_4$, 0.5 μM $CuSO_4$, 0.01 μM $CoCl_2$, 0.2 μM Na_2MoO_4, 1% (w/v) MES, and 1.5% (w/v) sucrose, solidified with 0.4% Gelrite pure (Kelco) and supplemented with 40 μM FeEDDHA. Plants were grown at 22°C under continuous light, 100 μmol $m^{-2}s^{-1}$ until time of collection. The pH was adjusted to various pH values as indicated. Media with a pH

above 7.0 were buffered with 1g/L MOPS; for pH 4.5 to 6.5 media 1g/L MES was used as buffering agent.

pH treatments

Ten-day-old plants were transferred from ES media pH 5.5 to plates containing media adjusted to pH 4.5 to 8.5 in increments of one unit. Additionally, plants were grown on plates supplemented with 3 mM NaHCO$_3$ (pH ~6.7). Roots exposed for 6 hours or 14 days to the varying pH conditions were isolated from the shoots and flash-frozen in liquid nitrogen.

RNA-seq analysis and definition of DEGs

Total RNA was isolated from roots of 10-day-old plants grown at optimal pH (5.5) or exposed for six-hour to pH 7.5 media using the RNeasy Plant Mini Kit (Qiagen). Three independent biological replicates were performed. Libraries for RNA-seq were prepared using the Illumina TruSeq RNA library Prep Kit (RS-122-2001, Illumina) according to the manufacturer's protocol. Four µg of total RNA were used for library construction. PolyA RNA was captured by oligodT beads and fragmented when eluted from the beads. First-strand cDNA was synthesized from fragmented RNA using reverse transcriptase (SuperScrip III, Cat. No. 18080-093, Invitrogen) and random primers. The cDNA was then converted into double stranded DNA using the reagents supplied with the kit. Reactions were cleaned up with Agencourt AMPure XP beads (Beckman Coulter Genomics). Libraries were end-repaired, adenylated at the 3' end, ligated with adapters, and amplified following the TruSeq[TM] RNA Sample Preparation v2 LS protocol. Finally, the products were purified and enriched with 10 cycles of PCR to create the final double-stranded cDNA library. For quality check, we used the BioRad QX200 Droplet Digital PCR EvaGreen supermix system (Cat. No. #1864034; BioRad, USA) and the Agilent High Sensitivity NGS Fragment Kit (1-6000 bp) (Cat. No. DNF-474-500; Agilent, USA). The prepared library was pooled for paired-end sequencing using Illumina the Novaseq 6000 at Taiwan Genome Industry Alliance Inc. (Taipei City, Taiwan) with 150 bp paired-ended sequence reads. RNAseq reads were pre-processed by trimmomatic (Bolger et al., 2014) for adapter removal (parameter: ILLUMINACLIP: TruSeq3-PE-2.fa:2:30:10:8:true MINLEN:80), where reads shorter than 80 bps were dropped. Passed reads were first mapped to transcript sequences of the Araport11 database using Bowtie2 (Langmead and Salzberg, 2012); only alignments of read pairs were accepted. The remaining reads were mapped to the Arabidopsis genome annotation (TAIR10) using BLAT (Kent, 2002). Read counts of genes were computed using the RackJ software package (https://rackj.sourceforge.net/) and normalized into log-count-per-million values using the TMM method (Robinson and Oshlack, 2010). Normalized RPKM values were inferred from the normalized log-count-per-million values. DEGs (differentially expressed genes) was identified as differentially expressed if the corresponding *P*-value was less than or equal to 0.05 and the fold-change was greater than two.

RT-qPCR

Frozen plant samples were ground to powder using a Qiagen Tissue Lyser II for three cycles of 30 secs. RNA extraction was performed using TRIzol® reagent; RNA was measured using a NanoDrop ND-1000 spectrophotometer. First-strand cDNA was synthesized using 1 µg RNA with the TOOLS Easy Fast RT Kit (Biotools). Three replicates of each sample measuring 10 µL reaction mixture made with AB SYBR Green PCR Master Mix (Applied Biosystems, Waltham, MA, USA) were used in the AB QuantStudio[TM] 12K Flex Real Time PCR System (Applied Biosystems) following a preset program. Transcripts were measured using the comparative C$_T$ ($\Delta\Delta$C$_T$) calculation method using multiple controls (EF1α and Tubulin). Graphs representing relative Expression ($2^{-\Delta\Delta CT}$) were built using GraphPad Prism 9 for Windows 64-bit. Primers used for RT-qPCR are listed in Supplemental Table 1.

Data analysis

Analysis of the Chen et al. (2021) data set was done by making comparisons of treated versus control samples using the Student's t-test with an adjusted P-value. This, and all the other data were filtered using a log2f old-change of |1|. Venn diagrams were assembled using Venn diagram <http://bioinformatics.psb.ugent.be/webtools/Venn/>; heatmaps were designed by TBTools (Chen et al., 2020) both were edited in Inkscape.

Co-expression analysis

To infer root-specific co-expression networks, a total of 1,194 root-specific RNA-seq data sets was downloaded from the Sequence Read Archive, hosted by the National Center for Biotechnology Information and normalized. Networks were constructed with the MACCU toolbox (Lin et al., 2011) based on pair-wise comparison of the co-expression relationships of Arabidopsis genes expressed in using Pearson coefficients as indicated in the figures. Co-expression networks were edited in Cytoscape (Shannon et al., 2003).

Plant growth characteristics

Fresh weight, rosette size, chlorophyll quantification

Whole shoots from 10- or 14-day-old plants grown on ES media with pH values ranging from pH 4.5 to 8.5 in increments of one or on media supplemented with NaHCO$_3$ were weighed and chlorophyll content was measured using extractions made with 80% acetone modified from the protocol described by Lichtenthaler (1987). Rosette diameter was determined using the Image J measure tool (Schindelin et al., 2012).

Results

Growth of Arabidopsis plants is strongly affected by media pH

To gain a better understanding regarding the responses of Arabidopsis plants to changes in external pH, we grew plants for a two-week period on media adjusted to pH values from 5.5 to 8.5. In addition, we added a treatment in which the medium was supplemented with 3 mM bicarbonate, resulting in a media pH of 6.7. As expected from an accession that is not derived from or adapted to calcareous or alkaline condition, plants grew best on slightly acidic media with pH values of 5.5 or 6.5 (Figure 1). Growth on media with pH 7.5 or 8.5 dramatically decreased growth and chlorophyll concentration of the plants (Figure 1). Bicarbonate-

treated plants showed a significant reduction in root and shoot weight, rosette diameter, and shoot-root ratio when compared to plants grown at comparable pH (6.5), indicative of effects that are independent of pH (Figure 1). Notably, plants grown on bicarbonate-supplemented media produced significantly longer roots than plants grown at pH 5.5 or 6.5, an observation which was also made for pH 7.5 plants. Stimulation of root growth by bicarbonate has been reported for a Zn-inefficient rice cultivar, whereas a Zn-efficient cultivar showed strong bicarbonate-induced root growth inhibition (Yang et al., 1994). Root growth correlated with the accumulation of citrate, which may have beneficial effects on root elongation, possibly associated with more efficient chelation of essential micronutrients. While we can only speculate as to why bicarbonate and alkalinity stimulated root elongation in the case of Arabidopsis. Increased citrate levels, possibly caused by higher ATPase activity and
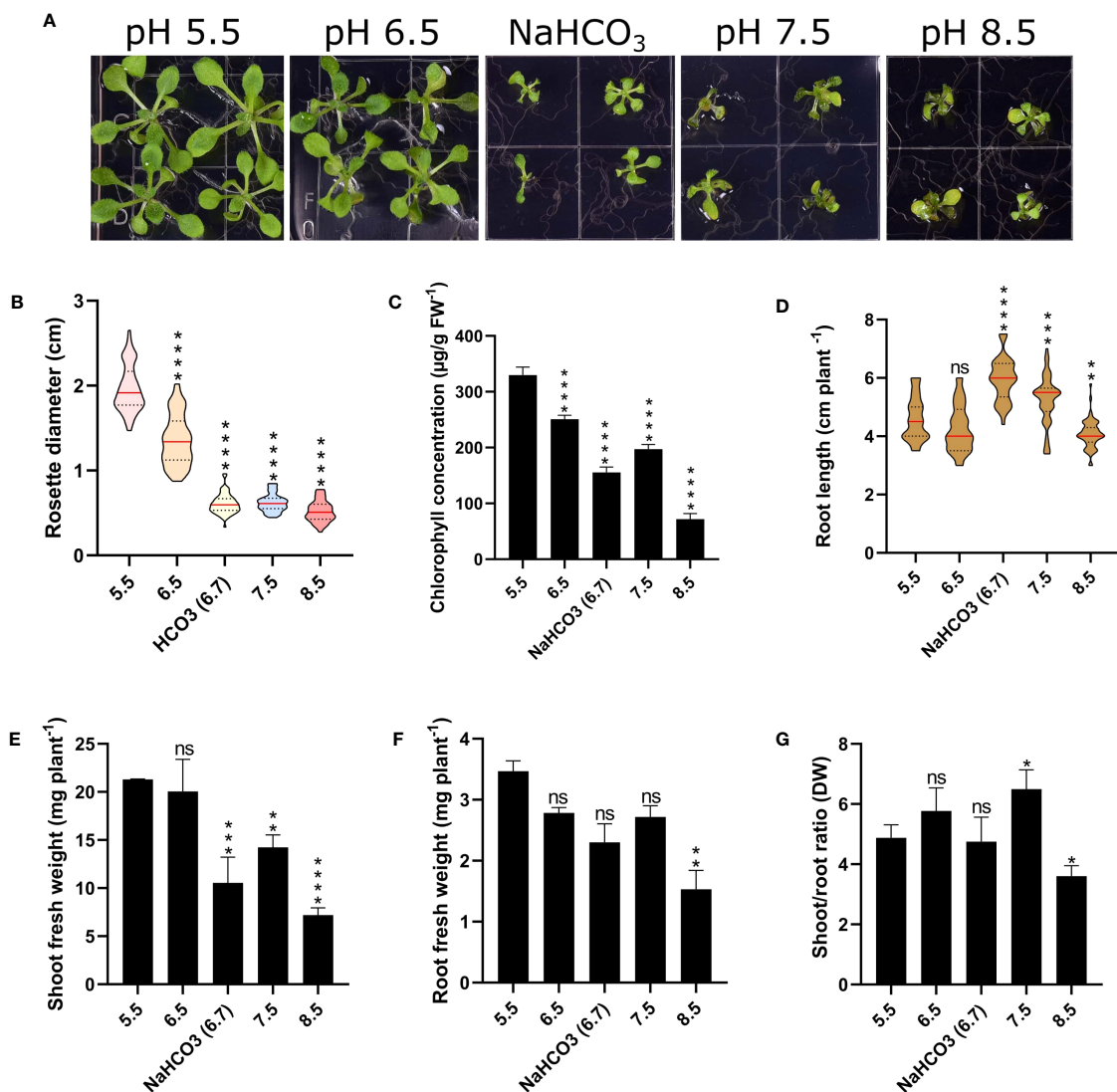
FIGURE 1
Phenotypic effects of varying media pH on plant growth. Plants were grown for 14 days under the various pH treatments. **(A)** Phenotypes. **(B)** Rosette diameter. **(C)** Chlorophyll concentration. **(D)** Root length. **(E)** Shoot fresh weight. **(F)** Root fresh weight (FW). **(G)** Shoot/root ratio (dry weight; DW). Values are mean $\pm$ SE of four replicates of four plants each. Statistical analysis was carried out using two-way Anova. Non-significant (ns) $P > 0.05$; $*P \leq 0.05$; $**P \leq 0.01$; $***P \leq 0.001$; $****P \leq 0.0001$.

subsequent accumulation of organic acids may be causative for the observed root elongation.
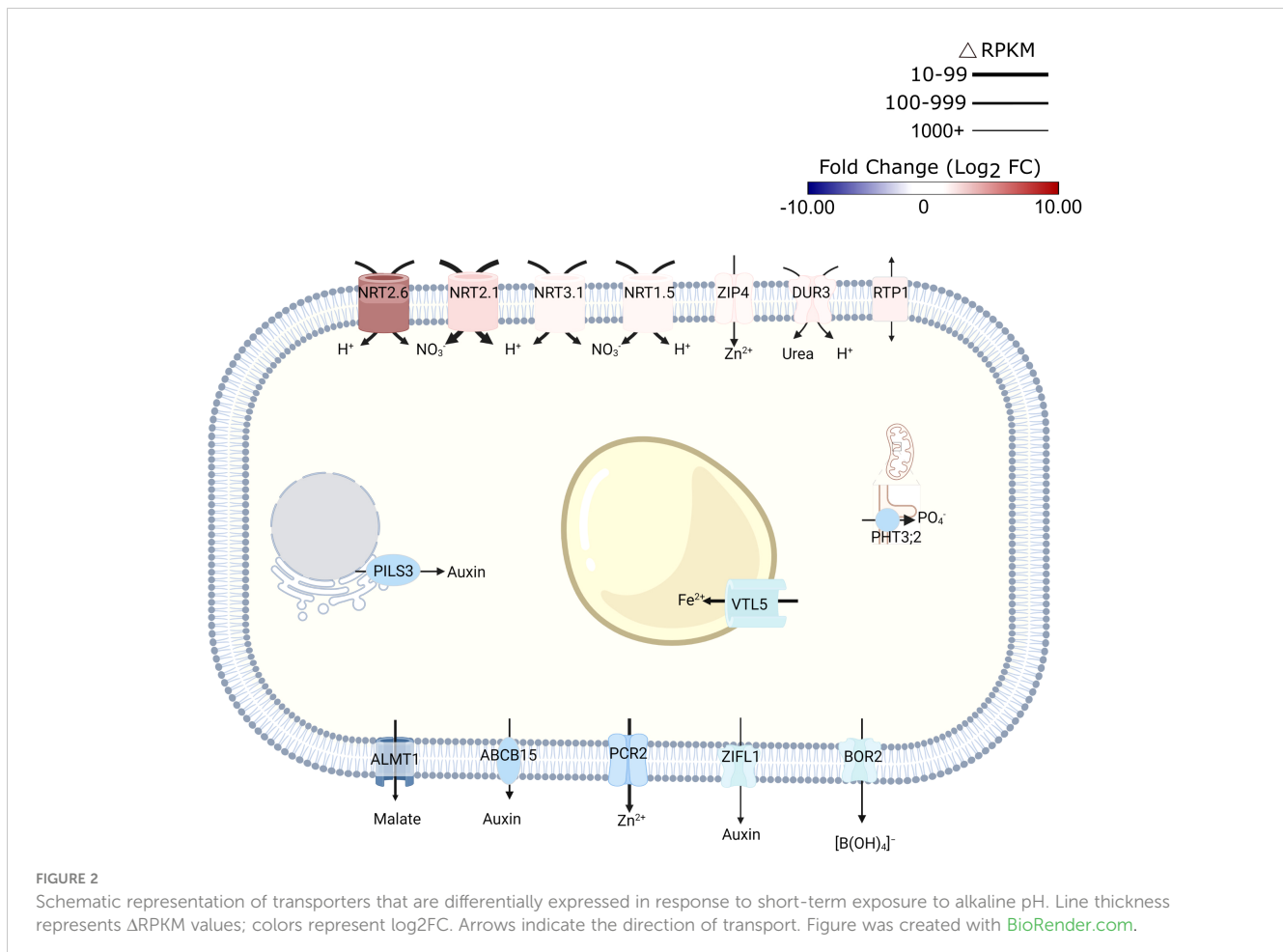
Exposure to high pH induces transport processes and tunes auxin homeostasis

To investigate the cause of growth cessation and leaf chlorosis of plants grown at alkaline pH, we transferred 10-day-old Arabidopsis Col-0 plants for six hours from slightly acidic media (pH 5.5) to media adjusted to pH 7.5. Roots were subjected to gene expression analysis via RT-qPCR or transcriptomic analysis via RNA-seq. For the latter approach, a total of 42-62 million paired-end reads with a length of 150 base pairs were acquired for each library using the Illumina NOVAseq 6000 sequencing system and aligned to the Araport 11 annotation of the Arabidopsis genome. In total, 419 genes were differentially expressed between plants grown on pH 5.5 media and media adjusted to pH 7.5. Gene ontology categorization of the differentially expressed genes highlights redox reactions, phenylpropanoid/lignin metabolism, response to salicylic acid, and fatty acid metabolism as overrepresented categories in this data set (Supplementary Figure S1).

Unexpectedly, exposure to alkalinity strongly induced a suite of high-affinity nitrate transporters (i.e., *NRT2.6.*, *NRT2.1*, *NRT2.4*, *NRT3.1* (*WR3*), and *NRT1.5*; Figure 2; Supplementary Table S2). Since NRT transporters are NO_3^-/H^+ cotransporters, the increased transcript levels are indicative of enhanced proton flux across the plasma membrane. Fitting this concept, also the expression of the rhizodermal urea/proton symporter *DUR3* (Kojima et al., 2007) was induced by elevated media pH (Figure 2). *NRT2.1* (Δ RPKM ~800) and *WR3* (Δ RPKM ~400), suggested to function as a NRT2.1-WR3 hetero-oligomer (Yong et al., 2010), were the largest contributors to the increase in anion/H^+-co-transport in terms of transcript levels (Figure 2). Since plants were grown on media supplemented with adequate nitrate levels, induction of nitrate transporters does not seem to indicate a low N-status of the plants. Rather, this observation suggests a massive enrichment of protons in the cytosol, a supposition that is corroborated by the observation that the mitochondrial (proton-coupled) phosphate transporter *PHT3.2* was among the most strongly downregulated genes after transfer to alkaline media (Figure 2). The proton/phosphate ratio for transporters of this type was estimated to be 2-4 (Młodzińska and Zboińska, 2016), suggesting rapid depletion of protons in the cytosol when this transporter is active.

Expression of the malate transporter *ALMT1* was reduced in response to high pH (Figure 2). Lower transcript abundance after transfer to pH 7.5 medium was also observed for the vacuolar iron transporter *VTL5*, presumably to avoid depletion of cytoplasmic iron. In addition to intracellular iron trafficking, uptake of Zn^{2+} from the soil

FIGURE 2
Schematic representation of transporters that are differentially expressed in response to short-term exposure to alkaline pH. Line thickness represents ΔRPKM values; colors represent log2FC. Arrows indicate the direction of transport. Figure was created with BioRender.com.

solution via ZIP4 was promoted at high pH; expression of the Zn^{2+} efflux protein *PCR2* was downregulated (Figure 2).

Consistent with the assumption that elevated pH is compromising growth, several genes involved in auxin signaling and transport were found to be affected by transfer to high pH media. This subset includes several —mostly upregulated— small auxin up-regulated RNA (SAUR) genes (i.e., *SAUR38*, *SAUR40*, *SAUR41*, *SAUR44*, *SAUR55*, and *SAUR64*), likely to facilitate cell expansion. A function specifically in this process has been described for SAUR40 and SAUR41 (Qiu et al., 2020). In addition, intracellular auxin homeostasis is affected through pH-dependent regulation of the auxin efflux genes *PILS3* and *ZIFL1* (Figure 2; Supplementary Table S2). Together, these observations suggest that transmembrane proton transport, metal transport, and auxin homeostasis are the processes that are most prominently reflected in transcriptomic profile changes upon exposure to high pH.

The expression of genes responsive to alkalinity is altered over a wide range of pH values

To obtain a more detailed picture on the pH-dependence of transcription, mRNA levels of selected genes from plants subjected to either short-term (6 hours) or long-term (14 days) growth on media with varied pH were determined by RT-qPCR (Figure 3). Gene expression appears to be highly responsive to short-term changes in external pH over a range of pH values to which plants are realistically exposed in their natural habitats. The nitrate transporters *NRT2.4*, *NRT2.6*, and *NRT3.1*, the plant intracellular Ras-group-related LRR *PIRL8*, the oxygenase *S8H*, and the DUF642 protein At2g41810 responded to the treatment with a continuous increase in transcript levels from low to high pH. A similar pattern was also observed for *EXPA17*, encoding an expansin that promotes lateral root formation (Lee and Kim, 2013), albeit expression of the gene was dramatically reduced at the highest pH. For another suite of genes comprising the laccase *LAC7*, the cytochrome P450 protein *CYP82C4*, the pathogen defense gene *MLO6*, the malate efflux transporter *ALMT1*, and the kinase *STRESS INDUCED FACTOR 1* (*SIF1*), an opposite pattern was recorded. *NRT1.1*, the main root nitrate transporter, showed a pronounced upregulation at low pH and a steep decrease in transcript levels at higher pH that plateaued at pH 5.5. Two of the tested genes, *SWEET12* and *SAUR44*, showed a more complex pattern (Figure 3). Gene expression patterns observed after 6 hours remained largely unchanged when plants were exposed to the various media for an extended experimental period of 14 days (Supplemental Figure S2). It should also be noted that the bicarbonate treatment resulted in gene expression changes that were in line with the pH of the media and not altered by the presence of the salt as such.

A comparison of the responses to alkalinity, iron deficiency, bicarbonate, and acidity identifies conserved gene clusters

In soils, elevated pH is generally associated with low availability of iron, excluding species with inefficient iron uptake systems from such habitats. To investigate whether exposure to elevated pH affects the iron status of the plants, we compared the transcriptome of pH 7.5 plants with the 'ferrome', a suite of genes that was found to be robustly modulated by iron supply across several studies (Hsieh et al., 2022). Whereas elevated pH strongly restricts the availability of iron *in situ*, in the current experimental set up iron mobility was sustained over a wide pH range by providing plants with the highly stable iron form FeEDDHA. A small subset of the ferrome genes was distinctly affected in roots of plants exposed to pH 7.5, possibly in anticipation of the iron shortage generally associated with increased pH (Figure 4). Pronounced upregulation was observed for the scopoletin hydroxylase *S8H*, a gene involved in the production of the iron-mobilizing coumarin fraxetin (Tsai et al., 2018; Gautam et al., 2021). Moreover, the vacuolar metal transporters *MTP8*, *IREG2*, and *VTL5*, the clade Ib transcription factor *bHLH100*, *LAC7*, and the H_2O_2-response gene *HRG1* were affected by the pH 7.5 treatment (Gong et al., 2021). Interestingly, a suite of 17 (mostly downregulated) ferrome genes was also modulated by low pH (Figure 4), underlining the link between pH and iron availability. *HRG1* is the sole ferrome gene that is part of both the low Fe and high pH data sets.

The presence of high bicarbonate levels adversely affects the uptake of essential mineral nutrients, including iron (Chen et al., 2021). To investigate how the response to bicarbonate relates to that to iron deficiency and high pH as such, we compared the pH 7.5 data set with previously published transcriptomic changes in roots from plants grown on bicarbonate-supplemented media (Chen et al., 2021). Bicarbonate-treated plants mounted a pronounced iron deficiency response, affecting the expression of a subset of 47 ferrome genes (44%; Figure 4). In addition, in this growth type a subset of 119 genes responsive to pH 7.5 was differentially expressed. The relatively large overlap of genes affected by bicarbonate with the pH 7.5 and iron deficiency transcriptomes suggests that bicarbonate-treated plants strongly respond to both high pH and iron deficiency in addition to the responses triggered by the presence of bicarbonate as such.

We further compared the pH 7.5 data set with the transcriptome of plants grown on circumneutral media supplemented with an immobile iron source (non-available iron; navFe). Only a relatively small subset of the ferrome genes was among the genes that were differentially expressed between plants grown on navFe media (pH 7.0) and those grown on iron-deplete media at acidic pH (5.5), but a much larger set of genes (41) was comprised in the pH 7.5 transcriptome (Figure 4). It thus appears that the response to high pH is substantially different from but partially overlapping with that observed in iron-deficient plants.

Since the expression of many pH 7.5 genes is also responsive to low pH, we included a data set derived from roots of plants exposed for 1 or 8 hours to pH 4.5 in the comparison (Lager et al., 2010). The transcriptomes of pH 7.5 and navFe plants showed a comparable percentage of genes responsive to low pH (19% and 21%, respectively; Figure 4). This number was lower for bicarbonate-treated (12%) and for iron-deficient plants (14%), indicating that in these growth types the response to iron deficiency and bicarbonate is dominant and the overall transcriptional changes are less affected by changes in media pH.
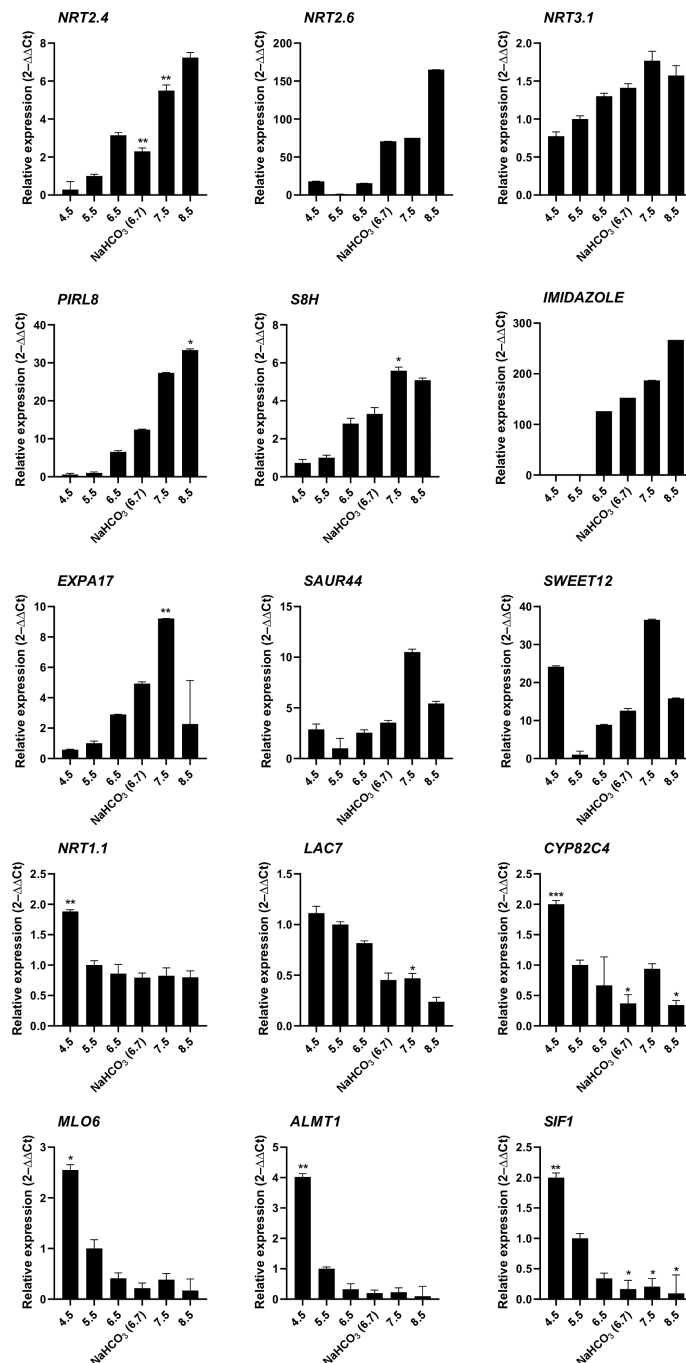
FIGURE 3

RT-qPCR analysis of the expression changes of selected genes in response to various pH treatments. Ten-day-old plants were transferred to solid media of varying pH for 6 hours. Gene expression values are normalized to EF1α and β-tubulin and calculated using the $2^{-\Delta\Delta Ct}$ method. Values are means $\pm$ standard deviation (SD) (n = 3). No asterisk P = 0.05; * P $\leq$ 0.05; ** P $\leq$ 0.01; *** P $\leq$ 0.001. Statistical differences were calculated between plants grown at pH 5.5 and those grown on media with other pH values.

Genes involved in growth, pH homeostasis, and defense adapt plants to alkalinity

To identify key players conferring calcicole behavior, we compared differentially expressed genes within the five data sets with stringent thresholds (3-fold change on a log2 basis) and under the condition that a gene is differentially regulated in at least three out of the five conditions under study (Figure 5). This conservative comparison highlighted three clusters of genes based on their susceptibility to a given suite of environmental conditions. The first group (cluster 1; 'cell elongation') comprises genes that were differentially expressed in all four pH-related treatments under investigation (i.e., pH 7.5, pH 4.5, navFe, and bicarbonate-treated plants). Three upregulated genes in this cluster encode proteins containing DUF642 domains. This domain is restricted to spermatophytes and putatively involved in homogalacturan
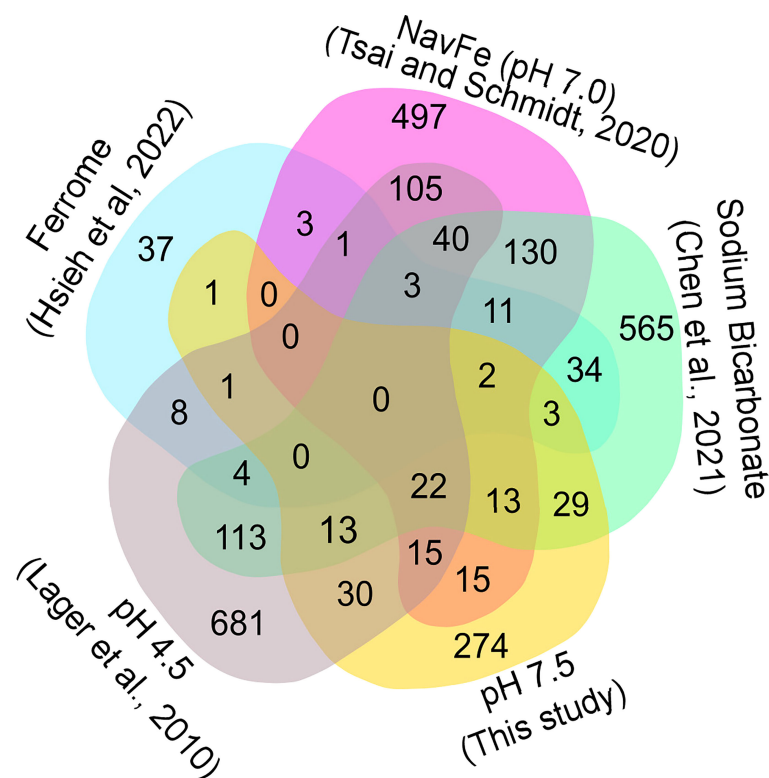
FIGURE 4
Venn diagram showing the commonalities of differentially expressed genes inferred from various RNA-seq derived data sets. Ferrome data are derived from Hsieh et al. (2022); NavFe data from Tsai and Schmidt (2020); data for bicarbonate-treated plants are taken from Chen et al. (2021) and normalized; pH 4.5 data are from Lager et al. (2010); data of pH 7.5 plants were generated in this study. The data were processed by trimming those that were statistically significant (*P* > 0.05) and differentially expressed with a log2 FC |1|.
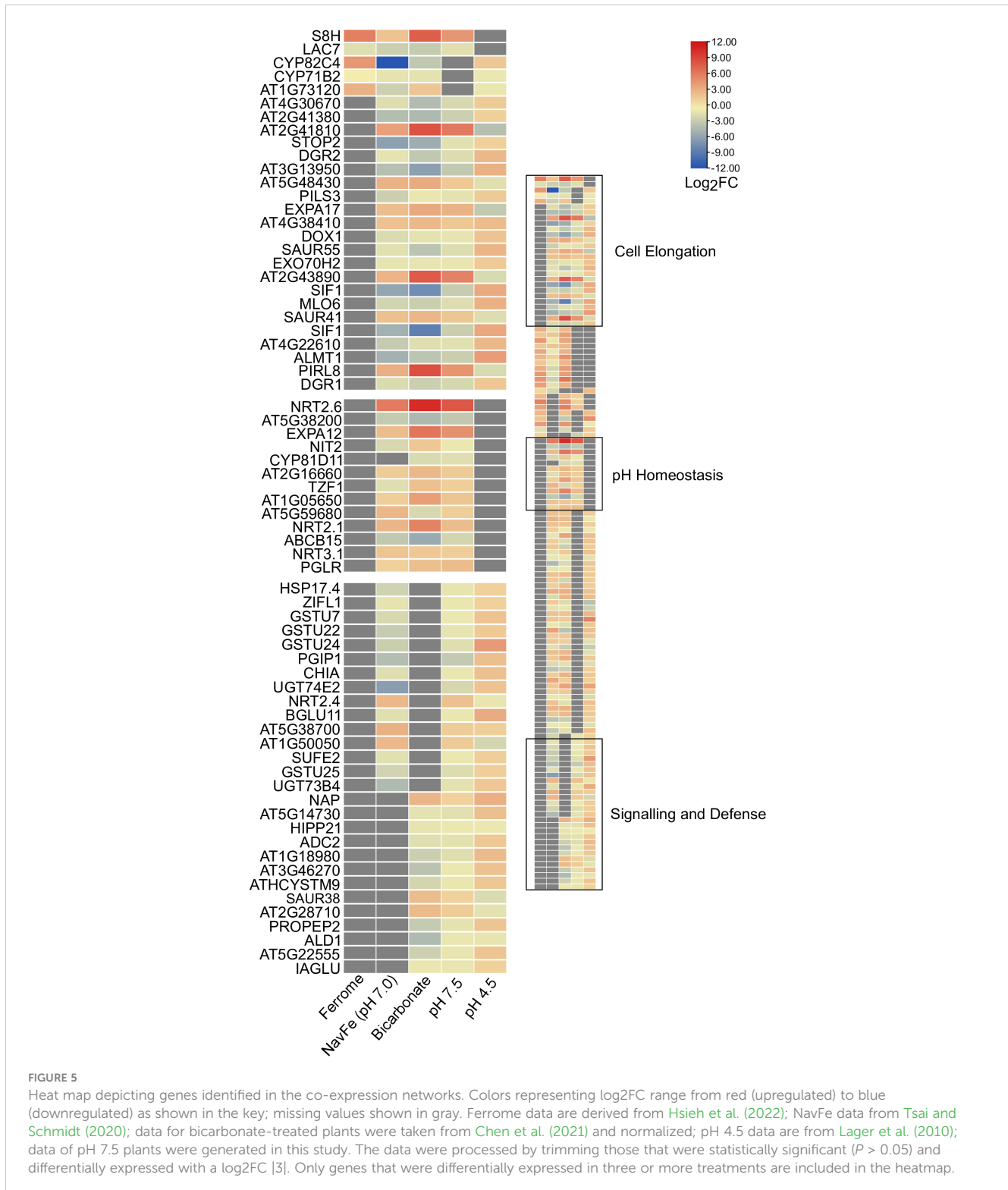
esterification, a process associated with cell wall loosening. Two other upregulated genes in this group, the pectin-lyase At2g43890 and the expansin *EXPA17,* also mediate cell wall-related processes. In addition, this cluster contains several genes involved in auxin homeostasis such as *SAUR41, SAUR44,* and the auxin transporter *PILS3.* Generally, genes affected by low pH were inversely regulated to those of the three high pH treatments. The cell elongation cluster also contains genes encoding putative signaling proteins or transcription factors that are largely undocumented such as *SIF1* and *PLANT INTRACELLULAR RAS GROUP-RELATED LRR 8* (*PIRL8*), representing the most dramatically regulated genes in this group. Notably, *PIRL8* was shown to be co-expressed with *EXPA17* and suggested to play a role in auxin-mediated lateral root growth (Hossain et al., 2022). *SENSITIVE TO PROTON RHIZOTOXICITY 2* (*STOP2*), a homolog of *STOP1,* encodes the only transcription factor in this module.

A second group (cluster 2; 'pH homeostasis') is comprised of genes that are solely regulated by treatments imposing elevated pH. Here, the two most strongly regulated genes within the pH 7.5 transcriptome are found, the nitrate transporter *NRT2.6* (up) and the nitrate-inducible class I glutamine amidotransferase-like superfamily protein At5g38200 (down). Furthermore, *NRT2.1, NRT3.1,* genes involved in cell wall modification, and an extra-cytoplasmatic LRR kinase (At5g59680) are part of this cluster.

The third module (cluster 3; 'sensing and defense') is comprised of genes responsive to both high and low pH (but not to iron) and contains two immune response-inducing secreted peptides, the CAP superfamily protein At1g50050, and the plant elicitor peptide *PEP2.* PEP1, a homolog of PEP2, was recently shown to sense extracellular alkalinity to induce immunity through binding to the receptor kinase PEPR (Liu et al., 2022a). The module also contains the so-far undocumented extra-cytoplasmatic receptor kinase At3g46270, which we named pHRK1 (pH-RECEPTOR KINASE 1). *pHRK1* and its homolog *pHRK2* (At3g46280) were both upregulated by elevated pH and previously found to be deregulated in *stop1* mutants (Sawaki et al., 2009).

Co-expression analysis uncovers a putative pH homeostasis module

To further elucidate the processes that acclimate plants to external pH, we constructed networks based on pair-wise comparison of the co-expression relationships of differentially expressed genes using a data base of a total of 1,194 root-specific normalized RNA-seq data sets from the Sequence Read Archive, hosted by the National Center for Biotechnology Information and the in-house developed MACCU toolbox (Lin et al., 2011). For pH 7.5 plants, the co-expression network features a subcluster

FIGURE 5
Heat map depicting genes identified in the co-expression networks. Colors representing log2FC range from red (upregulated) to blue (downregulated) as shown in the key; missing values shown in gray. Ferrome data are derived from Hsieh et al. (2022); NavFe data from Tsai and Schmidt (2020); data for bicarbonate-treated plants were taken from Chen et al. (2021) and normalized; pH 4.5 data are from Lager et al. (2010); data of pH 7.5 plants were generated in this study. The data were processed by trimming those that were statistically significant ($P > 0.05$) and differentially expressed with a log2FC |3|. Only genes that were differentially expressed in three or more treatments are included in the heatmap.

comprising *pHRK1*, *STOP2*, *SIF1*, *LAC7*, *ALMT1*, *SAUR55*, and the alpha-dioxygenase *DOX1*(Figure 6A). This sub-cluster appears to be conserved at low pH, but genes are generally regulated in the opposite direction (Figure 6B; Figure 7). Notably, this sub-cluster is also part of the co-expression network derived from bicarbonate-treated plants (Supplementary Figure S3). Some of the genes

observed in the network of pH 7.5 plants (i.e., *STOP2*, *EXPA17*, *LAC7*, *DOX1*, and *ALMT1*) are conserved in the network derived from navFe plants (Supplementary Figure S4). The co-expression analysis suggests that a suite of co-expressed and putatively co-regulated set of genes is involved in the adaptation to external pH over a wide range of proton concentrations.

Discussion

Bicarbonate, but not alkalinity as such triggers an iron deficiency response

Similar to what has been observed for plants responding to low pH (Lager et al., 2010), we show here that short-term exposure to moderate alkalinity leads to pronounced changes in the transcriptomic profile of Arabidopsis root cells. The phyto-availability of iron is closely related to soil pH and decreases dramatically at elevated pH. It can thus be speculated that alkalinity induces a response to iron deficiency, either as a consequence of 'true' iron depletion within the plant, caused by impaired uptake of iron, or in anticipation of the lower iron supply generally associated with alkaline substrates. This does, however, not seem to be the case; only a minor fraction of the ferrome genes was affected by raising the media pH. The small overlap of the two data sets does not seem to be caused by the short experimental period; a six-hour-transfer to iron-deplete media was sufficient to induce a much more pronounced iron stress response (Hsieh et al., 2022). The supposition that high pH and iron deficiency trigger separate signaling cascades is in line with the observation that restricting iron availability at circumneutral pH (navFe plants) does not simply intensify the expression of ferrome genes (Tsai and Schmidt, 2021). Rather, such treatment induced a separate, largely pH-dependent set of genes.

Long-term bicarbonate-treated plants (Chen et al., 2021) showed a more pronounced response to both iron deficiency and alkalinity than pH 7.5 plants, albeit the pH change induced by bicarbonate was less severe. Notably, short-term exposure to bicarbonate exerted a response that was not different from the influence of pH as such (this study). However, when we exposed plants to bicarbonate for a 14-day-period, growth was significantly more restricted than expected from the effect on pH, suggesting that the presence of bicarbonate enforces other constraints to growth and the homeostasis of mineral nutrients such as iron. The effect of bicarbonate on pH- and iron-responsive genes might be aggravated by the strong buffering effect of the salt, compromising compensatory measures to recalibrate both apoplastic and cytoplasmic pH as well as iron distribution and homeostasis.

External pH alters proton fluxes through modulation of anion/H$^+$ co-transporters

The free cytosolic H$^+$ concentration is in the sub-micromolar range (Wegner et al., 2021), and must be carefully balanced to avoid fluctuations in cytosolic pH and subsequent perturbations of cellular functions. Adjustment of cellular pH is thought to be mediated by a combination of H$^+$-producing and H$^+$-consuming reactions in concert with H$^+$ movements across the plasma membrane (Smith and Raven, 1979). Changes in the activity of NO_3^-/H$^+$ co-transporters significantly affect the pH of both the apoplast and the cytosol (Fan et al., 2016; Zhou et al., 2021). The current analysis suggests that dramatic changes in anion-coupled transmembrane H$^+$-fluxes are a general feature of plants exposed to alkaline pH; increased expression

of nitrate transporters was observed in pH 7.5, navFe, and bicarbonate-treated plants. Of note, induction of NRT homologs in response to alkaline pH was observed in a proteomic survey of sugar beet plants (Geng et al., 2021), suggesting that this response could be conserved across species. Upregulation of *NRT2.1* and *NRT3.1* was also reported for nitrate-treated plants (Vidal et al., 2013), a circumstance that was associated with the induction of enzymes related to the assimilation of nitrate such as the nitrate reductases NR1 and NR2. Conspicuously, in all three high pH treatments, the increase in transporter abundance does not seem to be correlated with nitrate assimilation. *NR* genes were either not regulated (in pH 7.5 and navFe plants) or dramatically repressed (in bicarbonate-treated plants) upon exposure to elevated pH (Supplementary Table S3). For example, *NR1* was 3-fold upregulated in nitrate-starved plants, but 5-fold downregulated upon exposure to bicarbonate. This observation resembles the regulation of other genes encoding enzymes involved in nitrate assimilation such as the glutamine synthetases *GLN2* and *GSR2* as well as the glutamate synthase *GLT1*, which are inversely regulated in nitrate-starved and bicarbonate-treated plants (Supplemental Table S3). Similar to pH 7.5 plants, the glutamine amidotransferase At5g38200 was strongly downregulated in bicarbonate plants but upregulated in nitrate-treated plants. It thus appears that the uptake, but not the assimilation of nitrate uptake is upregulated by high pH.

The supposition that proton homeostasis is the driving force behind the induction of nitrate transporters is supported by the pronounced upregulation of other anion/H$^+$ co-transporters such as *DUR2* and *NRT2.6*, a common observation across all high pH treatments. Further support for this assumption comes from the downregulation of intracellular anion/H$^+$ co-transporters such as *PHT3;2* (in pH 7.5 plants) and *SULTR3.5* (in bicarbonate-treated plants), which mediate transport processes that would deplete protons in the cytoplasm. *PHT3;2* and *SULTR3.5* are massively up-regulated in nitrate-starved plants, further supporting the idea that nitrate is triggering a response distinct from that to high pH. Also of note, expression of the nitrate exporter *NAXT1* was repressed in both nitrate-starved and bicarbonate-treated plants. NAXT1 protein abundance is induced by strong acidosis (Segonzac et al., 2007), further indicating that nitrate homeostasis is differently affected by external pH.

Acidic and alkaline pH induce distinct nitrate transporters

The nitrate transporter NRT1.1 is recruited to recalibrate apoplastic pH when plants are exposed to acidity (Ye et al., 2021). In line with this concept, our data confirm that acidic pH supports *NRT1.1* expression, an observation that has been reported earlier (Tsay et al., 1993). Notably, NRT1.1 activity was shown to impair the utilization of iron in leaves by alkalization of the apoplast (Ye et al., 2022). Since iron availability is severely restricted in an alkaline environment, a decrease rather than an increase in proton-coupled co-transport processes should be expected when plants are subjected to elevated pH. The rationale behind the —in terms of iron acquisition counterintuitive — induction of nitrate
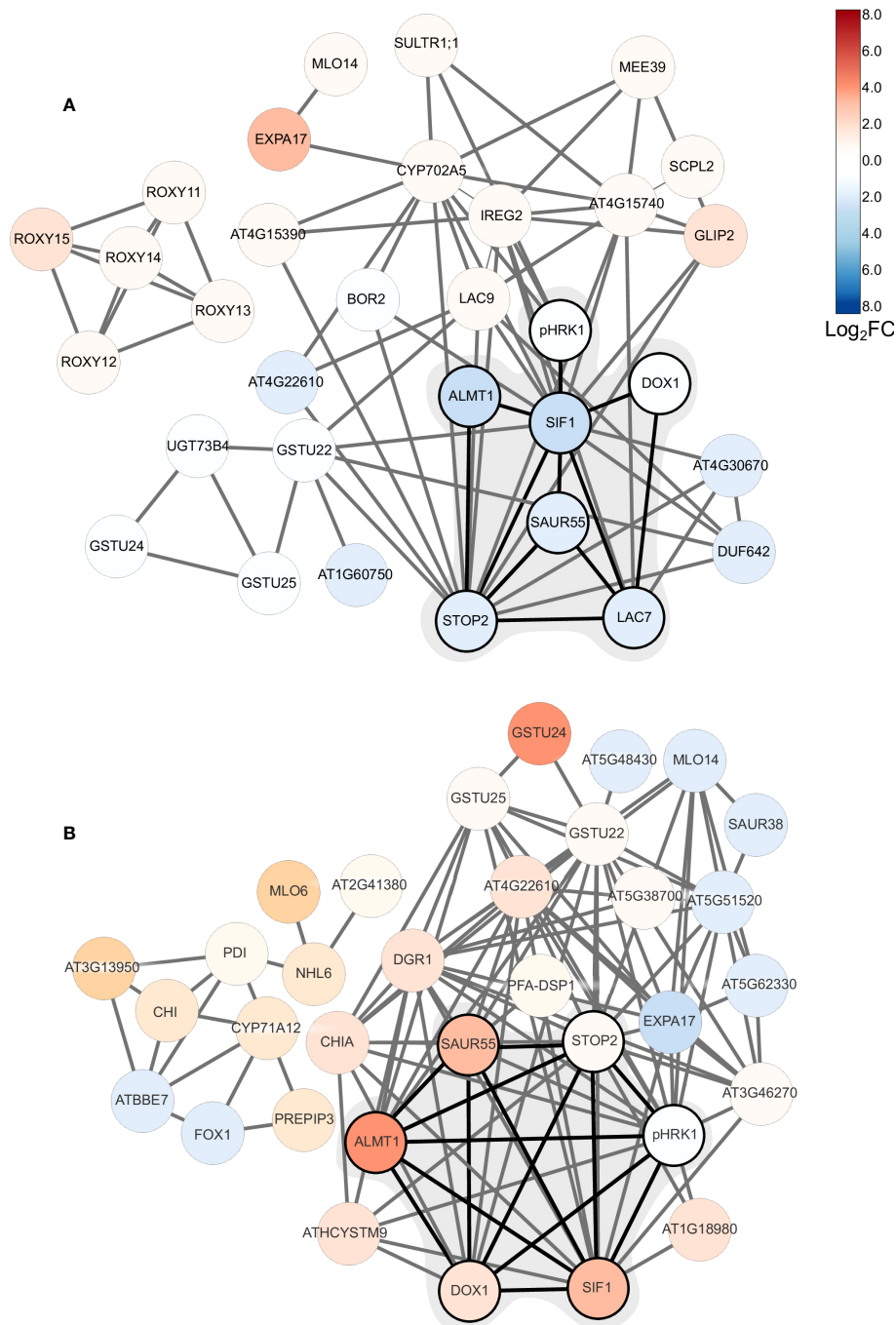
FIGURE 6
Co-expression network of DEGs from plants subjected to short-term changes in media pH. **(A)** pH 7.5 plants (this study); **(B)** plants subjected to pH 4.5 (Lager et al., 2010). Networks were generated using the in-house MACCU software package (Lin et al., 2011) against a data base comprising a suite of 1,194 normalized root-related RNA-seq data sets. Networks were constructed using a Pearson's correlation coefficient of <0.8 for pairwise expression of genes that were differentially expressed upon exposure to pH 7.5 or pH 4.5. Networks were drawn using Cytoscape. Log2C values are color coded according to the key.

transporters upon exposure to both low and high pH may be simply a matter of priorities. Cellular pH homeostasis might be difficult to achieve at an external pH of 7.5, which may increase cytosolic pH and massively disturb cellular functions without intervention. At acidic pH, an increase in apoplastic pH is essential to avoid cell damage due to Al^{3+} toxicity, but the protons taken up alongside nitrate are not severely affecting the pH gradient across the plasma

membrane since the external pH differs only by one pH unit from the optimal growth conditions for the calcifuge species *Arabidopsis thaliana*.

The answer to the question as to why different NO_3^- transporters are recruited at low and high pH (i.e., NRT1 vs NRT2) may lie in the fact that this differential recruitment upon high pH have distinct effects on root architecture. NRT2.1 was shown to promote lateral
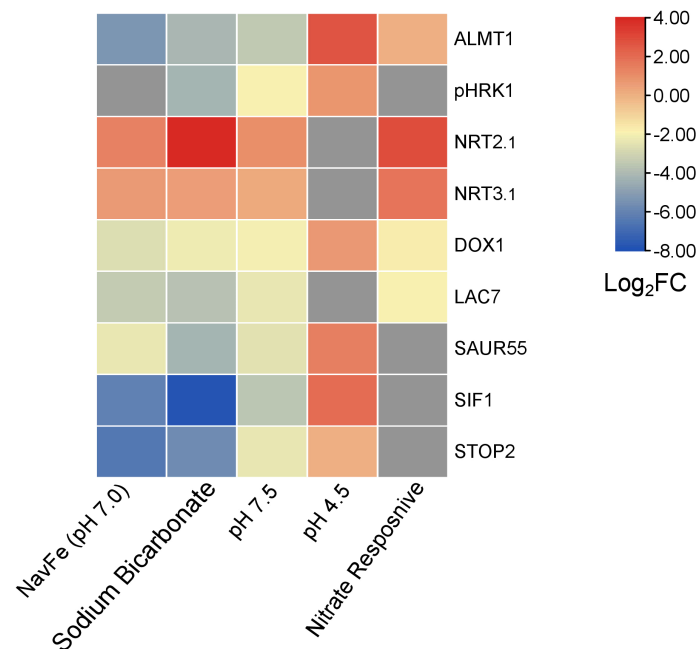
FIGURE 7
Heat map depicting genes that are differentially expressed in various treatments. NavFe data from Tsai and Schmidt (2020); data for bicarbonate-treated plants were taken from Chen et al. (2021) and normalized; pH 4.5 data are from Lager et al. (2010); nitrate-responsive data are from Vidal et al. (2013); data of pH 7.5 plants were generated in this study. The data was processed by trimming those that were statistically significant ($P > 0.05$) and differentially expressed with a log2FC |2|. Only genes that were differentially expressed in three or more treatments were included in the heatmap.

root initiation (Remans et al., 2006; van Gelderen et al., 2021), supporting topsoil foraging of phosphate, a scarce resource in a high pH environment. The effect of NRT2.1 on root development is, however, highly dependent on the N-status of the plant (Little et al., 2005), and may produce a distinct readout in calcareous soils. In rice, overexpression of *OsNRT2.1* enhanced elongation of primary roots (Naz et al., 2019), an effect that could counteract root growth inhibition at alkaline pH. It is thus tempting to assume that the recruitment of different NRT transporters in response to the external pH can adapt root growth and architecture to prevailing edaphic conditions. Crucially, in both pH 7.5 and bicarbonate-treated plants, a group of five nitrate-inducible thioredoxins (GRXS) were upregulated. Overexpression of *GRXS* genes was shown to suppress the expression of the nitrate transporters *NRT2.6* and *NRT3.1* (Ehrary et al., 2020). It can be assumed that *GRXS* genes are induced at high pH to balance the pronounced induction of genes involved in nitrate uptake in response to high pH.

A conserved gene module orchestrates root growth in response to external pH

The acid growth theory postulates that high apoplastic pH reduces growth by stiffening the cell wall and compromising cell elongation. How root growth is tuned in response to soil pH has yet to be elucidated. The current survey highlights a suite of robustly pH-regulated genes comprising *pHRK1*, *SIF1*, *LAC7*, *DOX1*, *SAUR55*, *STOP2*, and *ALMT1* that may play a role in pH-dependent growth regulation. Of particular interest is the extracellular receptor kinase

pHRK1, which is co-expressed with genes involved in iron uptake and homeostasis such as the putative iron sensors *BTSL1* and *BTSL2* (Supplemental Figure S5). The exact link between high pH signaling and iron metabolism remains to be established. pHRK1 has predicted interactions with the GRAS family transcription factor protein At5g19970, a member of the ferrome (Supplemental Figure S6). In line with such an interconnecting role, At5g19970 is responsive to iron deficiency, bicarbonate, nitrate, and navFe (although slightly exceeding the set P-value of 0.05 in the latter case). It thus appears that the responses to high pH, iron deficiency, and —to a certain degree— nitrate are interconnected by some promiscuous nodes that are orchestrating the responses to the plant to a given set of edaphic conditions (Figure 7).

The pronounced downregulation of *ALMT1* in all high pH treatments was an unexpected observation. Since the function of ALMT1 is Al^{3+} detoxification via malate secretion (Hoekenga et al., 2006; Kobayashi et al., 2007), one would not expect much difference in transcript abundance of this transporter between plants grown at optimal (pH 5.5) and alkaline pH. ALTM1 is, however, also critical in regulating root meristem activity and, thus, root growth. In response to phosphate deficiency, aberrant iron precipitation in the apoplast mediated by the multi-copper oxidase LPR2 and peroxidase-mediated redox cycling of iron lead to meristem exhaustion, cell wall stiffening, and subsequent growth arrest (Müller et al., 2015; Balzergue et al., 2017). In this setting, phosphate deficiency promotes the expression of *ALMT1* and represses primary root growth. Similar to phosphate deficiency, NH_4^+ toxicity leads to inhibition of primary root growth (Rogato et al., 2010). A forward genetic screen for mutants that are insensitive to NH_4^+-induced root growth cessation identified LPR2 as

being crucial for this process (Liu et al., 2022b). Similar to what has been observed under phosphate starvation, NH_4^+-induced root growth inhibition is accompanied by massive iron precipitation in the apoplast (here exclusively mediated by LPR2), which is upregulated by NH_4^+. NH_4^+-induced redox cycling of iron is associated with ROS formation, which in turn compromises sucrose transport in the phloem. Increasing NO_3^- uptake prevents aberrant iron deposition, thereby sustaining phloem function and sucrose supply to root cells. Phloem integrity is crucial for sustained root growth to counteract the inhibitory effect of high external pH. In fact, in the current survey, the sucrose transporters *SWEET11* and *SWEET12* were induced at high pH. Expression of the multi-copper oxidases *LAC7* and *LPR1/LPR2* is highest in the stele (http://bar.utoronto.ca/eplant), confined to the extracellular matrix and the proteins have similarities regarding their physiochemical properties (Supplementary Figure S7). It is tempting to assume that *ALMT1*, *LAC7*, and *DOX1* tune growth in response to and in concert with external pH. In this scenario, LAC7 would modulate root meristem activity under normal and acidic growth conditions, while the gene is strongly repressed at high pH, where root growth is hampered by reduced cell wall extensibility.

Support for this concept comes from another observation. Two nitrate-inducible GARP-type (NIGT) transcriptional repressors involved in the integration of N- and P-signaling, *HHO1* and *HRS1*, were found to be strongly downregulated in bicarbonate-treated plants. Phosphate deficiency induces the expression of *NIGT* genes, thereby inhibiting NRT2.1-mediated nitrate uptake and primary root growth (Medici et al., 2015). Notably, *HHO1* and *HRS1* are induced in nitrate-starved plants, possibly to regulate *NRT2.1* expression when N supply is restored. Together, these data suggest that downregulation of the *LAC7/DOX1/ALMT1* module at high pH adapt root meristem activity to the prevailing external pH.

Conclusions

The present survey allows us to infer a suite of adaptations that aid plants to thrive in alkaline substrates, comprising genes putatively involved in signaling extracellular pH and adjustment of intracellular pH. We further found that exposure to high pH modulates the transcript levels (as a proxy for altered activity) of anion/H^+ coupled transport processes in a way that secures the enrichment of protons in the cell interior, possibly to counteract alkalization of the cytoplasm. The regulation of root architecture by nitrate and nitrate transporters is complex and interlinked with auxin transport (Jia and von Wirén, 2020), making predictions regarding such changes in response to high pH vague with the information at hand. However, the consistency and robustness of the changes in the expression of genes involved in proton-coupled transport processes strongly imply that these changes adapt plants to alkalinity. Lastly, we show that a robustly co-expressed module comprising *ALMT1*, *LAC7*, and *DOX1* suppositionally regulates primary root growth in a pH-dependent manner. While the physiological role and ecological relevance of these adaptive processes awaits experimental validation, we believe that our study provides guidance for follow up research that will help to elucidate the molecular basis of calcicole behavior.

Data availability statement

The datasets presented in this study can be found in online repositories. The names of the repository/repositories and accession number(s) can be found below: https://www.ncbi.nlm.nih.gov/, SRR22018204~9.

Author contributions

MB, E-JH, H-HT, and AR conducted experiments and analyzed the data. WS conceived the project, analyzed the data and drafted the manuscript. All authors edited the manuscript and approved the final version of the draft.

Funding

Acknowledgments

Conflict of interest

The authors declare that the research was conducted in the absence of any commercial or financial relationships that could be construed as a potential conflict of interest.

Publisher's note

Supplementary material

The Supplementary Material for this article can be found online at: https://www.frontiersin.org/articles/10.3389/fpls.2023.1100701/full#supplementary-material

SUPPLEMENTARY FIGURE 1
Overrepresented GO categories in the pH 7.5 data set.

SUPPLEMENTARY FIGURE 2
RT-qPCR analysis of selected pH-dependent genes determined 14 days after exposure to the various treatments.

SUPPLEMENTARY FIGURE 3
Co-expression network of bicarbonate-treated plants.

SUPPLEMENTARY FIGURE 4
Co-expression network of navFe plants.

SUPPLEMENTARY FIGURE 5
Co-expression network around pHRK1.

SUPPLEMENTARY FIGURE 6
PPI network of pHRK1.

SUPPLEMENTARY FIGURE 7
Sequence alignment of the multi-copper oxidases LPR1, LPR2, and LAC7.

References

Aida, M., Beis, D., Heidstra, R., Willemsen, V., Blilou, I., Galinha, C., et al. (2004). The PLETHORA genes mediate patterning of the arabidopsis root stem cell niche. *Cell* 119, 109–120. doi: 10.1016/j.cell.2004.09.018

Balzergue, C., Dartevelle, T., Godon, C., Laugier, E., Meisrimler, C., Teulon, J. M., et al. (2017). Low phosphate activates STOP1-ALMT1 to rapidly inhibit root cell elongation. *Nat. Commun.* 8, 1–16. doi: 10.1038/ncomms15300

Bolger, A. M., Lohse, M., and Usadel, B. (2014). Trimmomatic: a flexible trimmer for illumina sequence data. *Bioinformatics* 30, 2114–2120. doi: 10.1093/bioinformatics/btu170

Chen, C., Chen, H., Zhang, Y., Thomas, H. R., Frank, M. H., He., Y., et al. (2020). TBtools: an integrative toolkit developed for interactive analyses of big biological data. *Mol. Plant* 13, 1194–1202. doi: 10.1016/j.molp.2020.06.009

Chen, J., Li, X., Ye, X., Guo, P., Hu, Z., Qi, G., et al. (2021). An s-ribonuclease binding protein EBS1 and brassinolide signaling are specifically required for arabidopsis tolerance to bicarbonate. *J. Exp. Bot.* 72, 1449–1459. doi: 10.1093/jxb/eraa524

Cosgrove, D. J. (2018). Diffuse growth of plant cell walls. *Plant Physiol.* 176, 16–27. doi: 10.1104/pp.17.01541

Ehrhary, A., Rosas, M., Carpinelli, S., Davalos, O., Cowling, C., Fernandez, F., et al. (2020). Glutaredoxin AtGRXS8 represses transcriptional and developmental responses to nitrate in *Arabidopsis thaliana* roots. *Plant Direct* 4, e00227. doi: 10.1002/pld3.227

Estelle, M. A., and Somerville, C. (1987). Auxin-resistant mutants of *Arabidopsis thaliana* with an altered morphology. *Mol. Gen. Genet.* 206, 200–206. doi: 10.1007/BF00333575

Fan, X., Tang, Z., Tan, Y., Zhang, Y., Luo, B., Yang, M., et al. (2016). Overexpression of a pH-sensitive nitrate transporter in rice increases crop yields. *Proc. Natl. Acad. Sci. U.S.A.* 113, 7118–7123. doi: 10.1073/pnas.1525184113

Gautam, C. K., Tsai, H. H., and Schmidt, W. (2021). IRONMAN tunes responses to iron deficiency in concert with environmental pH. *Plant Physiol.* 187, 1728–1745. doi: 10.1093/plphys/kiab329

Geng, G., Wang, G., Stevanato, P., Lv, C., Wang, Q., Yu, L., et al. (2021). Physiological and proteomic analysis of different molecular mechanisms of sugar beet response to acidic and alkaline pH environment. *Front. Plant Sci.* 1108. doi: 10.3389/fpls.2021.682799

Gjetting, S. K., Mahmood, K., Shabala, L., Kristensen, A., Shabala, S., Palmgren, M., et al. (2020). Evidence for multiple receptors mediating RALF-triggered Ca²⁺ signaling and proton pump inhibition. *Plant J.* 104, 433–446. doi: 10.1111/tpj.14935

Gong, F., Yao, Z., Liu, Y., Sun, M., and Peng, X. (2021). H2O2 response gene 1/2 are novel sensors or responders of H₂O₂ and involve in maintaining embryonic root meristem activity in *Arabidopsis thaliana*. *Plant Sci.* 310, 110981. doi: 10.1016/j.plantsci.2021.110981

Grime, J. P., and Hodgson, J. G. (1968). Investigation of the ecological significance of lime-chlorosis by means of largescale comparative experiments. *Brit Ecol. Soc. Symp.* 9, 67–99.

Hager, A., Menzel, H., and Krauss, A. (1971). Versuche und hypothese zur primärwirkung des auxins beim streckungswachstum. *Planta* 100, 47–75. doi: 10.1007/BF00386886

Hoekenga, O. A., Maron, L. G., Piñeros, M. A., Cançado, G. M., Shaff, J., Kobayashi, Y., et al. (2006). AtALMT1, which encodes a malate transporter, is identified as one of several genes critical for aluminum tolerance in arabidopsis. *Proc. Natl. Acad. Sci. U.S.A.* 103, 9738–9743. doi: 10.1073/pnas.0602868103

Hossain, M. F., Sultana, M. M., Tanaka, A., Dutta, A. K., Hachiya, T., and Nakagawa, T. (2022). Expression analysis of plant intracellular ras-group related leucine-rich repeat proteins (PIRLs) in *Arabidopsis thaliana*. *Biochem. Biophys. Rep.* 30, 101241. doi: 10.1016/j.bbrep.2022.101241

Hsieh, E. J., Lin, W. D., and Schmidt, W. (2022). Genomically hardwired regulation of gene activity orchestrates cellular iron homeostasis in arabidopsis. *RNA Biol.* 19, 143–161. doi: 10.1080/15476286.2021.2024024

Jia, Z., and von Wirén, N. (2020). Signaling pathways underlying nitrogen-dependent changes in root system architecture: from model to crop species. *J. Exp. Bot.* 71, 4393–4404. doi: 10.1093/jxb/eraa033

Kent, W. J. (2002). BLAT–the BLAST-like alignment tool. *Genome Res.* 2, 656–664. doi: 10.1101/gr.229202

Kobayashi, Y., Hoekenga, O. A., Itoh, H., Nakashima, M., Saito, S., Shaff, J. E., et al. (2007). Characterization of AtALMT1 expression in aluminum-inducible malate release and its role for rhizotoxic stress tolerance in arabidopsis. *Plant Physiol.* 145, 843–852. doi: 10.1104/pp.107.102335

Kojima, S., Bohner, A., Gassert, B., Yuan, L., and Wirén, N. V. (2007). AtDUR3 represents the major transporter for high-affinity urea transport across the plasma membrane of nitrogen-deficient arabidopsis roots. *Plant J.* 52, 30–40. doi: 10.1111/j.1365-313X.2007.03223.x

Lager, I. D. A., Andréasson, O. L. A., Dunbar, T. L., Andreasson, E., Escobar, M. A., and Rasmusson, A. G. (2010). Changes in external pH rapidly alter plant gene expression and modulate auxin and elicitor responses. *Plant Cell Environ.* 33, 1513–1528. doi: 10.1111/j.1365-3040.2010.02161.x

Langmead, B., and Salzberg, S. L. (2012). Fast gapped-read alignment with bowtie 2. *Nat. Meth.* 9, 357–359. doi: 10.1038/nmeth.1923

Lee, H. W., and Kim, J. (2013). EXPANSINA17 up-regulated by LBD18/ASL20 promotes lateral root formation during the auxin response. *Plant Cell Physiol.* 54, 1600–1611. doi: 10.1093/pcp/pct105

Li, L., Chen, H., Alotaibi, S. S., Pĕnčík, A., Adamowski, M., Novák, O., et al. (2022). RALF1 peptide triggers biphasic root growth inhibition upstream of auxin biosynthesis. *Proc. Natl. Acad. Sci. U.S.A.* 119, e2121058119. doi: 10.1073/pnas.2121058119

Li, L., Verstraeten, I., Roosjen, M., Takahashi, K., Rodriguez, L., Merrin, J., et al. (2021). Cell surface and intracellular auxin signalling for h⁺ fluxes in root growth. *Nature* 599, 273–277. doi: 10.1038/s41586-021-04037-6

Lichtenthaler, H. K. (1987). Chlorophylls and carotenoids: pigments of photosynthetic biomembranes. *Meth. Enzymol.* 148, 350–382. doi: 10.1016/0076-6879(87)48036-1

Lin, W., Zhou, X., Tang, W., Takahashi, K., Pan, X., Dai, J., et al. (2021). TMK-based cell-surface auxin signalling activates cell-wall acidification. *Nature.* 599 (7884), 278–282. doi: 10.1038/s41586-021-03976-4

Lin, W. D., Liao, Y. Y., Yang, T. J., Pan, C. Y., Buckhout, T. J., and Schmidt, W. (2011). Coexpression-based clustering of arabidopsis root genes predicts functional modules in early phosphate deficiency signaling. *Plant Physiol.* 155, 1383–1402. doi: 10.1104/pp.110.166520

Little, D. Y., Rao, H., Oliva, S., Daniel-Vedele, F., Krapp, A., and Malamy, J. E. (2005). The putative high-affinity nitrate transporter NRT2. 1 represses lateral root initiation in response to nutritional cues. *Proc. Natl. Acad. Sci. U.S.A.* 102, 13693–13698. doi: 10.1073/pnas.0504219102

Liu, L., Song, W., Huang, S., Jiang, K., Moriwaki, Y., Wang, Y., et al. (2022a). Extracellular pH sensing by plant cell-surface peptide-receptor complexes. *Cell* 185, 3341–3355. doi: 10.1016/j.cell.2022.07.012

Liu, X. X., Zhang, H. H., Zhu, Q. Y., Ye, J. Y., Zhu, Y. X., Jing, X. T., et al. (2022b). Phloem iron remodels root development in response to ammonium as the major nitrogen source. *Nat. Commun.* 13, 1–16. doi: 10.1038/s41467-022-28261-4

Martinière, A., Gibrat, R., Sentenac, H., Dumont, X., Gaillard, I., and Paris, N. (2018). Uncovering pH at both sides of the root plasma membrane interface using noninvasive imaging. *Proc. Natl. Acad. Sci. U.S.A.* 115, 6488–6493. doi: 10.1073/pnas.1721769115

Medici, A., Marshall-Colon, A., Ronzier, E., Szponarski, W., Wang, R., Gojon, A., et al. (2015). AtNIGT1/HRS1 integrates nitrate and phosphate signals at the arabidopsis root tip. *Nat. Commun.* 6, 1–11. doi: 10.1038/ncomms7274

Młodzińska, E., and Zboińska, M. (2016). Phosphate uptake and allocation–a closer look at *Arabidopsis thaliana* l. and *Oryza sativa* l. *Front. Plant Sci.* 7, 1198. doi: 10.3389/fpls.2016.01198

Müller, J., Toev, T., Heisters, M., Teller, J., Moore, K. L., Hause, G., et al. (2015). Iron-dependent callose deposition adjusts root meristem maintenance to phosphate availability. *Dev. Cell* 33, 216–230. doi: 10.1016/j.devcel.2015.02.007

Naz, M., Luo, B., Guo, X., Li, B., Chen, J., and Fan, X. (2019). Overexpression of nitrate transporter OsNRT2. 1 enhances nitrate-dependent root elongation. *Genes* 10, 290. doi: 10.3390/genes10040290

Pearce, G., Moura, D. S., Stratmann, J., and Ryan, C. A. (2001). RALF, a 5-kDa ubiquitous polypeptide in plants, arrests root growth and development. *Proc. Natl. Acad. Sci. U.S.A.* 98, 12843–12847. doi: 10.1073/pnas.201416998

Qiu, T., Qi, M., Ding, X., Zheng, Y., Zhou, T., Chen, Y., et al. (2020). The SAUR41 subfamily of SMALL AUXIN UP RNA genes is abscisic acid inducible to modulate cell expansion and salt tolerance in *Arabidopsis thaliana* seedlings. *Ann. Bot.* 125, 805–819. doi: 10.1093/aob/mcz160

Remans, T., Nacry, P., Pervent, M., Filleur, S., Diatloff, E., Mounier, E., et al. (2006). The Arabidopsis NRT1. 1 transporter participates in the signaling pathway triggering root colonization of nitrate-rich patches. *Proc. Natl. Acad. Sci. U.S.A.* 103, 19206–19211. doi: 10.1073/pnas.0605275103

Robinson, M. D., and Oshlack, A. (2010). A scaling normalization method for differential expression analysis of RNA-seq data. *Genome Biol.* 11, R25. doi: 10.1186/gb-2010-11-3-r25

Rogato, A., D'Apuzzo, E., Barbulova, A., Omrane, S., Parlati, A., Carfagna, S., et al. (2010). Characterization of a developmental root response caused by external ammonium supply in *Lotus japonicus. Plant Physiol.* 154, 784–795. doi: 10.1104/pp.110.160309

Sawaki, Y., Iuchi, S., Kobayashi, Y., Kobayashi, Y., Ikka, T., Sakurai, N., et al. (2009). STOP1 regulates multiple genes that protect arabidopsis from proton and aluminum toxicities. *Plant Physiol.* 150, 281–294. doi: 10.1104/pp.108.134700

Schindelin, J., Arganda-Carreras, I., Frise, E., Kaynig, V., Longair, M., Pietzsch, T., et al. (2012). Fiji: An open-source platform for biological-image analysis. *Nat. Meth.* 9, 676–682. doi: 10.1038/nmeth.2019

Segonzac, C., Boyer, J. C., Ipotesi, E., Szponarski, W., Tillard, P., Touraine, B., et al. (2007). Nitrate efflux at the root plasma membrane: identification of an arabidopsis excretion transporter. *Plant Cell* 19, 3760–3777. doi: 10.1105/tpc.106.048173

Shannon, P., Markiel, A., Ozier, O., Baliga, N. S., Wang, J. T., Ramage, D., et al. (2003). Cytoscape: a software environment for integrated models of biomolecular interaction networks. *Genome Res.* 13, 2498–2504. doi: 10.1101/gr.1239303

Smith, F. A., and Raven, J. A. (1979). Intracellular pH and its regulation. *Annu. Rev. Plant Biol.* 30, 289–311. doi: 10.1146/annurev.pp.30.060179.001445

Tsai, H. H., Rodríguez-Celma, J., Lan, P., Wu, Y. C., Vélez-Bermúdez, I. C., and Schmidt, W. (2018). Scopoletin 8-hydroxylase-mediated fraxetin production is crucial for iron mobilization. *Plant Physiol.* 177, 194–207. doi: 10.1104/pp.18.00178

Tsai, HH, and Schmidt, W. (2020). pH-dependent transcriptional profile changes in iron-deficient Arabidopsis roots. *BMC Genomics.* 21 (1), 694. doi: 10.1186/s12864-020-07116-6

Tsai, H. H., and Schmidt, W. (2021). The enigma of environmental pH sensing in plants. *Nat. Plants* 7, 106–115. doi: 10.1038/s41477-020-00831-8

Tsay, Y. F., Schroeder, J. I., Feldmann, K. A., and Crawford, N. M. (1993). The herbicide sensitivity gene CHL1 of arabidopsis encodes a nitrate-inducible nitrate transporter. *Cell* 72, 705–713. doi: 10.1016/0092-8674(93)90399-B

van Gelderen, K., Kang, C., Li, P., and Pierik, R. (2021). Regulation of lateral root development by shoot-sensed far-red light via HY5 is nitrate-dependent and involves the NRT2. 1 nitrate transporter. *Front. Plant Sci.* 12, 660870. doi: 10.3389/fpls.2021.660870

Vidal, E. A., Moyano, T. C., Riveras, E., Contreras-López, O., and Gutiérrez, R. A. (2013). Systems approaches map regulatory networks downstream of the auxin receptor AFB3 in the nitrate response of *Arabidopsis thaliana* roots . *Proc. Natl. Acad. Sci. U.S.A.* 110, 12840–12845. doi: 10.1073/pnas.1310937110

Wegner, L. H., Li, X., Zhang, J., Yu, M., Shabala, S., and Hao, Z. (2021). Biochemical and biophysical pH clamp controlling net h$^+$ efflux across the plasma membrane of plant cells. *New Phytol.* 230, 408–415. doi: 10.1111/nph.17176

Ye, J. Y., Tian, W. H., Zhou, M., Zhu, Q. Y., Du, W. X., Zhu, Y. X., et al. (2021). STOP1 activates NRT1. 1-mediated nitrate uptake to create a favorable rhizospheric pH for plant adaptation to acidity. *Plant Cell* 33, 3658–3674. doi: 10.1093/plcell/koab226

Ye, J. Y., Zhou, M., Zhu, Q. Y., Zhu, Y. X., Du, W. X., Liu, X. X., et al. (2022). Inhibition of shoot-expressed NRT1. 1 improves reutilization of apoplastic iron under iron-deficient conditions. *Plant J.* 12, 549–564. doi: 10.1111/tpj.15967

Yong, Z., Kotur, Z., and Glass, A. D. (2010). Characterization of an intact two-component high-affinity nitrate transporter from arabidopsis roots. *Plant J.* 63, 739–748. doi: 10.1111/j.1365-313X.2010.04278.x

Zhang, H., Yu, F., Xie, P., Sun, S., Qiao, X., Tang, S., et al. (2023). A gγ protein regulates alkaline sensitivity in crops. *Science* 379, eade416. doi: 10.1126/science.ade8416

Zhou, J. Y., Hao, D. L., and Yang, G. Z. (2021). Regulation of cytosolic pH: the contributions of plant plasma membrane h$^+$-ATPases and multiple transporters. *Int. J. Mol. Sci.* 22, 12998. doi: 10.3390/ijms222312998